UvA-DARE (Digital Academic Repository)

Time Scale for Adiabaticity Breakdown in Driven Many-Body Systems and Orthogonality Catastrophe

Lychkovskiy, O.; Gamayun, O.; Cheianov, V.

Link to publication

Supplement

1. Quantum speed limit and relation between orthogonality catastrophe and adiabaticity

In contrast to the main text, in the present section we use time, not λ, to parameterize the instantaneous ground state of the system, Φ_t, and the evolving state of the system, Ψ_t. The former is a solution of the Schrodinger's stationary equation

$$\hat{H}_{\lambda(t)} \, \Phi_t = E_{\lambda(t)} \, \Phi_t, \tag{S1}$$

while the latter satisfies the Schrodinger's equation

$$i \frac{\partial}{\partial t} \Psi_t = \hat{H}_{\lambda(t)} \, \Psi_t \tag{S2}$$

with the initial condition $\Psi_0 = \Phi_0$. Here $\lambda(t)$ can be an arbitrary smooth function of time. We will also slightly abuse the notations and write $\mathcal{R}(t) \equiv \mathcal{R}\left(\lambda(t)\right)$.

1.1. Relation between orthogonality catastrophe and adiabaticity

Here we prove the inequality (8) of the main text which relates the orthogonality overlap $\mathcal{C}(\lambda)$ with the adiabatic fidelity $\mathcal{F}(\lambda)$. We rewrite it as follows:

$$\left|\mathcal{F}\left(\lambda(t)\right) - \mathcal{C}\left(\lambda(t)\right)\right| \leq \mathcal{R}(t) \equiv \int_0^t \sqrt{\langle\Psi_0|\hat{H}_{\lambda(t')}^2|\Psi_0\rangle - \langle\Psi_0|\hat{H}_{\lambda(t')}|\Psi_0\rangle^2} \, dt'. \tag{S3}$$

Here the integration is performed over the path in the parameter space parameterised by time, and t corresponds to the end point λ of this path.

In order to prove the bound (S3) we employ the quantum speed limit (QSL) in the following form:

$$D(\Psi_0, \Psi_t) \leq \frac{2}{\pi} \mathcal{R}(t), \tag{S4}$$

where D defined by Eq. (9) of the main text is a distance on the Hilbert space known as Bures angle, quantum angle or Fubini-Study metric. The QSL (S4) is a direct consequence of a more general result by Pfeifer [1, 2]. A detailed derivation of eq. (S4) can be found in the next subsection.

Combining the QSL (S4) with the triangle inequality

$$\left|D(\Phi_t, \Psi_0) - D(\Phi_t, \Psi_t)\right| \leq D(\Psi_0, \Psi_t) \tag{S5}$$

and taking into account that $\Psi_0 = \Phi_0$, one gets

$$\left|D(\Phi_t, \Phi_0) - D(\Phi_t, \Psi_t)\right| \leq \frac{2}{\pi}\mathcal{R}(t). \tag{S6}$$

Finally, one obtains the inequality (S3) from the inequality (S6) by observing that

$$\left|x^2 - y^2\right| \leq \left|\arccos x - \arccos y\right| \quad \text{for all} \quad |x| \leq 1, \ |y| \leq 1. \tag{S7}$$

One may wonder what is the reason for using the Bures angle distance instead of e.g. a more conventional trace distance, $D_{\text{tr}}(\Psi, \Phi) \equiv \sqrt{1 - |\langle\Phi|\Psi\rangle|^2}$. It is easy to see that the trace distance is bounded by the Bures angle, $D_{\text{tr}}(\Psi, \Phi) < (\pi/2)D(\Psi, \Phi)$, and thus eq. (S4) entails the following (weaker) version of the QSL,

$$D_{tr}(\Psi_0, \Psi_t) \leq \mathcal{R}(t). \tag{S8}$$

However, if we try to move forward with this QSL instead of eq. (S4), we get an extra factor 2 in the r.h.s. of the bound (S3). Let us show this. Using (S8) and triangle inequality for the trace distance, one obtains an analog of (S6):

$$\left|D_{tr}(\Phi_t, \Phi_0) - D_{tr}(\Phi_t, \Psi_t)\right| \leq \mathcal{R}(t). \tag{S9}$$

Now one has to relate the l.h.s. of this inequality with the l.h.s. of inequality (S3). This amounts to relating $|\sqrt{1 - x^2} - \sqrt{1 - y^2}|$ with $|x^2 - y^2|$, and at this point extra 2 emerges. This is because one can only guarantee that

$$\left|x^2 - y^2\right| \leq 2|\sqrt{1 - x^2} - \sqrt{1 - y^2}|, \tag{S10}$$

compare to eq. (S7).

1.2. Quantum speed limit

Here we derive the QSL limit (S4) from a result by Pfeifer [1, 2] which reads

$$\sin_* \left(\arcsin |\langle F|\Psi_0\rangle| - \mathcal{R}(t) \right) \leq |\langle F|\Psi_t\rangle| \leq \sin_* \left(\arcsin |\langle F|\Psi_0\rangle| + \mathcal{R}(t) \right). \tag{S11}$$

Here F is an arbitrary auxiliary state and

$$\sin_* x \equiv \begin{cases} 0, & x < 0, \\ \sin x, & 0 \leq x \leq \pi/2, \\ 1, & x > \pi/2. \end{cases} \tag{S12}$$

Noting that $\arcsin x + \arccos x = \pi/2$ and $\sin_*(\pi/2 - x) = \cos_* x$ with

$$\cos_* x \equiv \begin{cases} 1, & x < 0, \\ \cos x, & 0 \leq x \leq \pi/2, \\ 0, & x > \pi/2, \end{cases} \tag{S13}$$

one can rewrite (S11) as

$$\cos_* \left(\arccos |\langle F|\Psi_0\rangle| + \mathcal{R}(t) \right) \leq |\langle F|\Psi_t\rangle| \leq \cos_* \left(\arccos |\langle F|\Psi_0\rangle| - \mathcal{R}(t) \right). \tag{S14}$$

Taking into account that

$$\arccos(\cos_* x) = \begin{cases} 0, & x < 0, \\ x, & 0 \leq x \leq \pi/2, \\ \pi/2, & x > \pi/2, \end{cases} \tag{S15}$$

one rewrites eq. (S14) in terms of the Bures angle:

$$\max\{D(F, \Psi_0) - \frac{2}{\pi}\mathcal{R}(t), 0\} \leq D(F, \Psi_t) \leq \min\{D(F, \Psi_0) + \frac{2}{\pi}\mathcal{R}(t), 1\}. \tag{S16}$$

Employing obvious relations $\min\{x, y\} \leq x$ and $\max\{x, y\} \geq x$ one reduces (S16) to a more compact, though slightly more rough inequality,

$$|D(F, \Psi_t) - D(F, \Psi_0)| \leq \frac{2}{\pi}\mathcal{R}(t). \tag{S17}$$

Choosing $F = \Psi_0$ one obtains the QSL (S4).

It should be noted that another choice, $F = \Phi_t$, directly reduces the inequality (S17) (along with the condition $\Psi_0 = \Phi_0$) to the inequality (S6). Such a direct route which apparently dispenses with the triangle inequality is possible because Pfeifer's rather sophisticated result has, in fact, a more broad scope than elementary versions of the quantum speed limit and contains the triangle inequality built in.

2. Rice-Mele model

2.1. Eigenstates and eigenenergies

The transformation

$$a_j = \frac{1}{\sqrt{N}} \sum_k e^{ikj} a_k, \quad b_j = \frac{1}{\sqrt{N}} \sum_k e^{ikj} b_k, \quad k = \frac{2\pi}{N}l, \quad l = -\frac{N}{2}+1, -\frac{N}{2}+2, ..., \frac{N}{2}, \tag{S18}$$

where N is assumed to be even, allows one to represent the Rice-Mele Hamiltonian, eq. (12) in the main text, as a sum of N commuting terms,

$$\hat{H}_{\mathrm{RM}} = \sum_k (a_k^\dagger \, b_k^\dagger) \begin{pmatrix} \Delta & -(J+U)-(J-U)e^{ik} \\ -(J+U)-(J-U)e^{-ik} & -\Delta \end{pmatrix} \begin{pmatrix} a_k \\ b_k \end{pmatrix}. \tag{S19}$$

Observe that $n_k \equiv a_k^\dagger a_k + b_k^\dagger b_k$ is conserved for each k. We assume half-filling, i.e. that the total number of particles equals N. In this case the ground state of the Hamiltonian for any values of (J, U, Δ) is an eigenstate of n_k with the eigenvalue

equal to 1, and this is maintained throughout the evolution. Restricting the Hamiltonian (S19) to the corresponding subspace one obtains an effective Hamiltonian of N noninteracting spins,

$$\hat{H}_{\text{RM}} = \sum_k \boldsymbol{p}_k \cdot \boldsymbol{\sigma}_k, \qquad \boldsymbol{p}_k = \begin{pmatrix} -(J+U) - (J-U)\cos k \\ (J-U)\sin k \\ \Delta \end{pmatrix}, \tag{S20}$$

where $\boldsymbol{\sigma}$ is a vector consisting of three Pauli matrices. Each two-level Hamiltonian $\hat{H}_k \equiv \boldsymbol{p}_k \cdot \boldsymbol{\sigma}_k$ has two eigenstates $|\chi_k^{\pm}\rangle$ and eigenenergies $\varepsilon_k^{\pm}$,

$$\rho_k^{\pm} \equiv |\chi_k^{\pm}\rangle\langle\chi_k^{\pm}| = \frac{1}{2}(1 \pm \frac{1}{|\boldsymbol{p}_k|}\boldsymbol{p}_k \cdot \boldsymbol{\sigma}_k), \qquad \varepsilon_k^{\pm} = \pm\sqrt{2(J^2+U^2) + \Delta^2 + 2(J^2-U^2)\cos k}. \tag{S21}$$

The ground state of the whole system is the product of N single-spin eigenstates, $|\Phi\rangle = \prod_k \otimes |\chi_k^-\rangle$ while the ground state energy is the sum of corresponding eigenenergies, $E = \sum_k \varepsilon_k^-$.

2.2. Orthogonality catastrophe

Here we consider the orthogonality catastrophe induced by changing the parameters of the Hamiltonian (J, U, Δ) along some trajectory parameterized by λ. This is to say that (J, U, Δ) and thus vectors $\boldsymbol{p}_k$ are functions of λ. In contrast to the main text, we do not employ the convention that $\lambda = 0$ at $t = 0$.

The orthogonality overlap for a single spin reads

$$\mathfrak{c}_k(\lambda', \lambda) \equiv |\langle\chi_k^-(\lambda')|\chi_k^-(\lambda)\rangle|^2 = \text{tr}(\rho_k^-(\lambda)\rho_k^-(\lambda')) = \frac{1}{2}(1 + \frac{\boldsymbol{p}_k(\lambda) \cdot \boldsymbol{p}_k(\lambda')}{|\boldsymbol{p}_k(\lambda)| \, |\boldsymbol{p}_k(\lambda')|}). \tag{S22}$$

The orthogonality overlap for the whole many-body system is given by

$$\mathcal{C}(\lambda', \lambda; N) \equiv |\langle\Phi_{\lambda'}|\Phi_\lambda\rangle|^2 = \exp\left(-\sum_k \log \frac{1}{\mathfrak{c}_k}\right). \tag{S23}$$

Further,

$$C_N = \sum_k c_k \quad \text{with} \quad c_k \equiv -\frac{1}{2}\left(\frac{\partial^2}{\partial\lambda^2}\log \mathfrak{c}_k(\lambda', \lambda)\right)\Big|_{\lambda'=\lambda} = \frac{1}{4}\left(\frac{\partial_\lambda \boldsymbol{p}_k \cdot \partial_\lambda \boldsymbol{p}_k}{|\boldsymbol{p}_k|^2} - \frac{(\boldsymbol{p}_k \cdot \partial_\lambda \boldsymbol{p}_k)^2}{|\boldsymbol{p}_k|^4}\right). \tag{S24}$$

This equation along with eq. (S20) enables one to calculate C_N for any point of any trajectory in the parameter space of the Rice-Mele model. For example, for $J, U = \text{const}$, $\Delta = \lambda E_R$ one obtains

$$c_k = \frac{1}{8}\frac{1}{J^2 + U^2 + (J^2-U^2)\cos k} \tag{S25}$$

and

$$C_N = \frac{N E_R^2}{16 JU}. \tag{S26}$$

2.3. Quantum uncertainty of the driving potential

To deal with general trajectories we define the driving term as

$$\hat{V} \equiv \partial_\lambda \hat{H}_\lambda, \tag{S27}$$

which is consistent with the definition adopted in the main text. For the Rice-Mele model

$$\hat{V} = \sum_k \partial_\lambda \boldsymbol{p}_k \cdot \boldsymbol{\sigma}_k. \tag{S28}$$
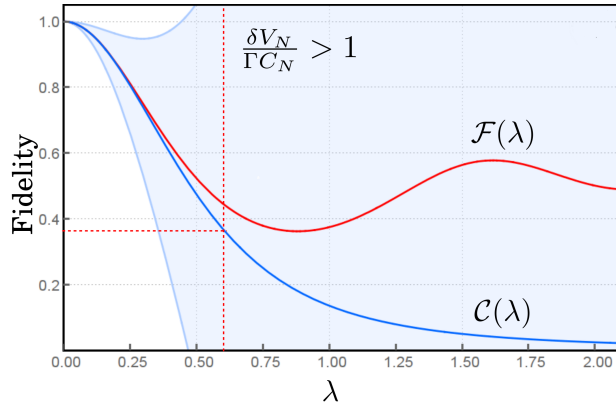
FIG. 1. Evolution of the ground state fidelity in the parameter space of the Hamiltonian (S19) for $N = 10$ particles. The fidelity $\mathcal{F}$ is shown as a solid red curve, while the overlap function $\mathcal{C}$ is shown as a solid blue curve. The shaded region is the one, which has to contain the $\mathcal{F}(\lambda)$ curve due to the inequality (S3). For $N = 10$ the inequality (S3) does not impose a meaningful upper bound on the fidelity, and therefore has nothing to say about the relationship between the fidelity and the orthogonality catastrophe. The parameters used read $J = 0.4E_R$, $U = 0.4E_R$ and $\Delta = \lambda E_R$ with $\lambda = \Gamma t$ and $\Gamma = 0.7E_R$. For the recoil energy $E_R = 6.4 \text{ ms}^{-1}$ these coincide with the parameters of the effective Hamiltonian describing the optical lattice in the experiment Ref. [3] at the $\Delta = 0$ point of the pumping cycle.

Since the ground state is of the product form, the quantum uncertainty of $\hat{V}$ is expressed through individual uncertainties of states of single spins:

$$\delta V^2 = \sum_k \left(\text{tr}\left(\rho_k^- \left(\partial_\lambda \boldsymbol{p}_k \cdot \boldsymbol{\sigma}_k\right)^2\right) - \left(\text{tr}\left(\rho_k^- \partial_\lambda \boldsymbol{p}_k \cdot \boldsymbol{\sigma}_k\right)\right)^2 \right) = \sum_k \left(|\partial_\lambda \boldsymbol{p}_k|^2 - \frac{(\boldsymbol{p}_k \cdot \partial_\lambda \boldsymbol{p}_k)^2}{|\boldsymbol{p}_k|^2} \right). \tag{S29}$$

This equation along with eq. (S20) allows one to calculate δV_N for any point of any trajectory in the parameter space of the Rice-Mele model. For example, for $J, U = \text{const}$, $\Delta = \lambda E_R$ one gets

$$\delta V_N^{\text{RM}} = \sqrt{N} E_R. \tag{S30}$$

With the knowledge of C_N and δV_N one can make practical use of the inequality (8) of the main text, or, alternatively, inequality (S3). For a fixed Γ the r.h.s. of this inequality inevitably diminishes with growing N, leading to $\mathcal{F}(\lambda) \simeq \mathcal{C}(\lambda)$, as illustrated in Fig. 2 (a) of the main text. The opposite situation when the r.h.s. of (S3) is large and thus the inequality (S3) is inconclusive is illustrated in Fig. 1.

2.4. Current and transferred charge

The current flowing between the l'th and $(l+1)$'th elementary cell reads

$$\hat{j}_l = i(J - U) \sum_{l=1}^{N} (b_{l+1}^\dagger a_l - a_l^\dagger b_{l+1}). \tag{S31}$$

Due to translation invariance of the Hamiltonian and the initial state the current is the same for all cells. It is convenient to define an average current,

$$\hat{j} \equiv \frac{1}{N} \sum_{l=0}^{N} \hat{j}_l, \tag{S32}$$

and then express it in terms of a_k, b_k:

$$\hat{j} = \frac{i}{N} \sum_k (a_k^\dagger \; b_k^\dagger) \begin{pmatrix} 0 & -(J-U)e^{ik} \\ (J-U)e^{-ik} & 0 \end{pmatrix} \begin{pmatrix} a_k \\ b_k \end{pmatrix}. \tag{S33}$$

In terms of spin variables the current can be written as

$$\hat{j} = \frac{1}{N} \sum_k \hat{j}_k \quad \text{with} \quad \hat{j}_k = \boldsymbol{j}_k \cdot \boldsymbol{\sigma}_k, \qquad \boldsymbol{j}_k = \begin{pmatrix} (J-U)\sin k \\ (J-U)\cos k \\ 0 \end{pmatrix}, \tag{S34}$$
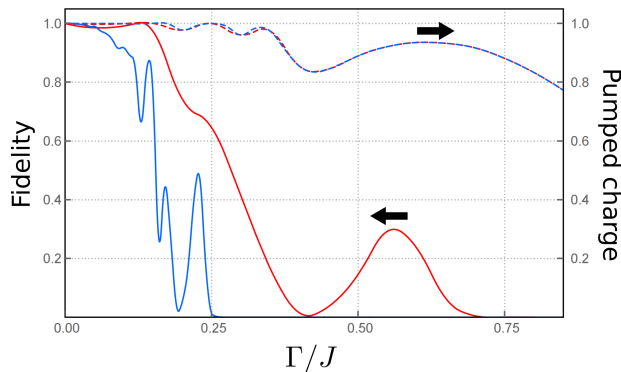
FIG. 2. Fidelity (solid curves) and pumped charge (dashed curves) after a single cycle in the Rice-Mele realisation of the Thouless pump, eq. (S19). The trajectory of the cycle is given by $\Delta = (J/2)\sin\lambda$, $U = (J/2)\cos\lambda$ with $\lambda = \Gamma t$. The system is initiated in equilibrium. Red and blue curves correspond to $N = 100$ and $N = 1000$ fermions in a lattice, respectively. One can see that the charge transferred in a single cycle hardly depends on the number of particles for $N \gtrsim 100$ while the fidelity decays more rapidly for larger N.

The pumped charge is the integral of the quantum average of this current over the elapsed time:

$$Q(t) = \int_0^t dt' \, \langle \Psi_{t'} | \hat{j} | \Psi_{t'} \rangle. \tag{S35}$$

Thanks to eq. (S20) and factorized initial condition $\Psi_0 = \Phi_0 = \prod_k \chi_k^-$, eq. (S35) can be written as

$$Q(t) = \int_0^t dt' \prod_k \langle \chi_k(t') | \hat{j}_k | \chi_k(t') \rangle, \tag{S36}$$

where $\chi_k(t)$ is found from the Schrodinger equation

$$i \, \partial_t \, \chi_k(t) = (\boldsymbol{p}_k(t) \cdot \boldsymbol{\sigma}_k) \, \chi_k(t). \tag{S37}$$

In the context of Thouless pumping we enquire how much charge is transferred per cycle immediately after the first cycle is over, and in the steady state regime. To answer the former question we calculate $Q(t)$ by solving the Schrodinger equations (S37) numerically. The result is illustrated in Fig. 2. The latter question is addressed by counting the number of right- and left- moving excitations produced during the cycle. To this end we define the average population of the excited state with the quasimomentum k,

$$w_k = \langle \chi_k(T) | \frac{1}{2}(1 + \boldsymbol{p}_k(T) \cdot \boldsymbol{\sigma}_k) | \chi_k(T) \rangle. \tag{S38}$$

Remind that $\chi_k(T)$ should be found numerically from the Schrodinger equation (S37). Taking into account that $\boldsymbol{p}_k(T) = \boldsymbol{p}_k(0)$ this can be rewritten with the use of eq. (S21) as

$$w_k = |\langle \chi_k^+ | \chi_k(T) \rangle|^2. \tag{S39}$$

The sign of the group velocity of the excitations, $\partial(\varepsilon_k^+ - \varepsilon_k^-)/\partial k$, coincides with the sign of k for $-\pi < k < \pi$, as is clear from eq. (S21). Therefore the charge transferred from left to right per cycle in the steady state, ΔQ, reads

$$\Delta Q = \sum_{0 < k < \pi} w_k - \sum_{-\pi < k < 0} w_k. \tag{S40}$$

[1] Peter Pfeifer, "How fast can a quantum state change with time?" Physical review letters **70**, 3365 (1993).

[2] Peter Pfeifer and Jürg Fröhlich, "Generalized time-energy uncertainty relations and bounds on lifetimes of resonances,"

Reviews of Modern Physics **67**, 759 (1995).

[3] Shuta Nakajima, Takafumi Tomita, Shintaro Taie, Tomohiro Ichinose, Hideki Ozawa, Lei Wang, Matthias Troyer, and Yoshiro Takahashi, "Topological thouless pumping of ultracold fermions," Nature Physics (2016).